Magnetospatial dispersion of semiconductor quantum wells

L. V. Kotova,[1,2] V. N. Kats,[1] A. V. Platonov,[1] V. P. Kochereshko,[1] R. André,[3] and L. E. Golub[1]
[1]*Ioffe Institute, St. Petersburg 194021, Russia*
[2]*ITMO University, St. Petersburg 197101, Russia*
[3]*Université Grenoble Alpes, CNRS, Institut NEEL, Grenoble F-38000, France*

(Received 1 December 2017; published 5 March 2018)

Polarization conversion of light reflected from quantum wells governed by both magnetic field and light propagation direction is observed. We demonstrate that the polarization conversion is caused by the magnetospatial dispersion in quantum wells which manifests itself in the reflection coefficient contribution bilinear in the in-plane components of the magnetic field and the light wave vector. The magnetospatial dispersion is shown to arise due to structure inversion asymmetry of the quantum wells. The effect is resonantly enhanced in the vicinity of the heavy-hole exciton. We show that microscopically the magnetospatial dispersion is caused by the mixing of heavy- and light-hole states in the quantum well due to both orbital effect of the magnetic field and the in-plane hole motion. The degree of the structure inversion asymmetry is determined for GaAs/AlGaAs and CdTe quantum wells.

DOI: 10.1103/PhysRevB.97.125302

I. INTRODUCTION

Magneto-optical phenomena attract great attention due to their importance for both fundamental science and applications in optoelectronics [1]. Magneto-optical properties of low-dimensional systems such as quantum wells (QWs) and other heterostructures are especially interesting in this sense. All magneto-optical phenomena are useful to classify considering an expansion of the optical response functions over the magnetic field strength $\boldsymbol{B}$ and the light wave vector $\boldsymbol{q}$. For the susceptibility $\hat{\chi}$ relating the dielectric polarization $\boldsymbol{P}$ and the electric field $\boldsymbol{E}$ as $\boldsymbol{P} = \hat{\chi}\boldsymbol{E}$, we have to the lowest order in $\boldsymbol{B}$ and $\boldsymbol{q}$

$$\chi_{ij}(\boldsymbol{B},\boldsymbol{q}) = \chi^0_{ij} + S_{ijk}B_k + i\gamma_{ijk}q_k + C_{ijkl}B_k q_l. \quad (1)$$

Here the first term describes birefringence, and the next contribution given by the tensor $\hat{S}$ describes the well-known Faraday and magneto-optical Kerr (MOKE) effects. The term with the tensor $\hat{\gamma}$ describes gyrotropic phenomena [2]. Nonzero components of $\hat{\gamma}$ are allowed by symmetry only in systems lacking a space inversion center. Moreover, some components of a vector and a pseudovector should belong to the same representation of the space symmetry group of the studied system. In QW structures, gyrotropy can be caused by both bulk and structure inversion asymmetry [3]. The effects caused by the linear in the wave vector terms in Eq. (1) are special because they result in a difference of velocities of the circularly polarized waves propagating in opposite directions. In particular, the tensor $\hat{\gamma}$ describes the optical activity of QWs demonstrated recently [4].

The term with the tensor $\hat{C}$ bilinear in both the light wave vector $\boldsymbol{q}$ and the magnetic field $\boldsymbol{B}$ describes the effect of magnetospatial dispersion (MSD). MSD is present in gyrotropic media only. In contrast to the Faraday and magneto-optical Kerr effects, MSD is governed by the light propagation direction, and its symmetry is different from the pure $\boldsymbol{B}$-linear part. For example, the terms linear in both $\boldsymbol{q}$ and $\boldsymbol{B}$ are invariant at time inversion operation while the $\boldsymbol{B}$-linear contributions change their sign. Therefore they contribute to different effects and can be distinguished by a proper choice of experimental geometry. MSD has been demonstrated in reflection and transmission experiments on various bulk semiconductors: GaAs [5], CdSe [6], ZnTe, CdTe [7], CdZnTe [8], thin films [9], magnetic semiconductors [10], as well as in the second optical harmonics generation in ZnO [11]. Here we report on the observation of MSD in quantum well structures. It is well known that MSD effects are strongly enhanced in the vicinity of exciton resonances [2,6,8,9]. We study the heavy-hole exciton resonance in the geometry where the magnetic field $\boldsymbol{B}$ lies the plane of the QW and the light incidence plane contains $\boldsymbol{B}$, Fig. 1(a). We detect a polarization conversion of the reflected light. In particular, the *s* or *p* linearly polarized light is reflected elliptically polarized. The effect of pure magnetic field given by the second term in Eq. (1) would be an appearance of the orthogonal electrical polarization due to the longitudinal MOKE. However this effect can occur if the excited optical transition is allowed in both polarizations perpendicular to the magnetic field. This is not the case for the heavy-hole exciton which has zero dipole momentum normal to the QW plane. In contrast, allowance for the exciton motion in the QW plane ($\boldsymbol{q}_\parallel \neq 0$) leads to the last term in Eq. (1). Microscopically it comes from the mixing of the heavy- and light-hole excitons in the QW at finite hole wave vectors in the magnetic field. This mixing caused by both the magnetic field and hole motion represents the microscopic mechanism of MSD.

The MSD induced conversion coefficient linear in both $\boldsymbol{B}$ and $\boldsymbol{q}$ is observed for both III-V and II-VI asymmetrical quantum wells. We demonstrate that MSD exists due to structure inversion asymmetry (SIA) of the QWs under study. The developed microscopic theory allowed us to explain quantitatively the amplitude of the MSD-induced reflection signal and to determine the SIA degree in the studied samples.

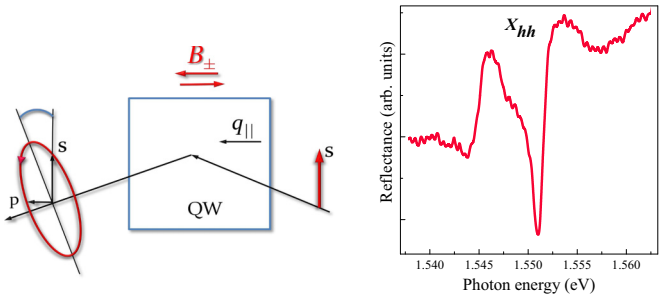

FIG. 1. (a) Experimental setup: s-polarized light at oblique incidence on a QW, magnetic field in the QW plane. The reflected light is elliptically polarized due to magnetospatial dispersion. (b) Reflectance spectrum measured from the GaAs asymmetric heterostructure in the vicinity of the X_{hh} resonance at the incidence angle $\theta_0 = 27^\circ$.

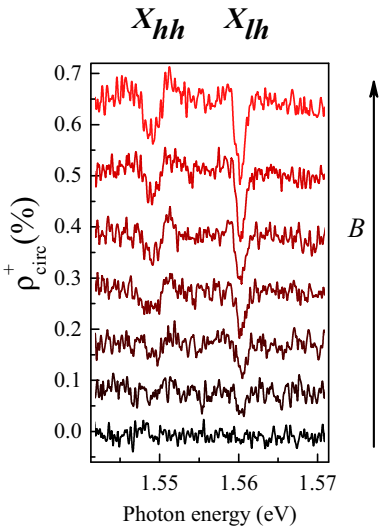

FIG. 2. Odd in $\boldsymbol{B}$ part of the circular polarization of light reflected from the GaAs/AlGaAs asymmetric heterostructure. The heavy-hole (X_{hh}) and light-hole (X_{lh}) exciton resonances are shown. Magnetic field $B = 0.05, 0.2, 0.4, 0.5, 0.6, 0.8$ and 1 T (from bottom to top, the spectra are vertically shifted for clarity). Temperature $T = 3$ K.

II. EXPERIMENT

For observation of the MSD effect, the sample should have a substantial degree of SIA. In QW structures, SIA can be induced in two ways: (i) the heteropotential can have a triangular shape or (ii) left and right barriers of a rectangular QW have different heights. In this work both possibilities are realized. A triangular GaAs/AlGaAs QW was grown by the molecular beam epitaxy (MBE) method on a semi-insulating substrate in the [001] direction. The structure contains a 200-nm-wide $Al_{0.28}Ga_{0.72}As$ barrier followed by the 8-nm-wide QW. Then the other sloping barrier was grown with Al concentration smoothly increasing from 4% to 28% on a layer of width 27 nm. The structure design is identical to that of the sample used in Ref. [12] where the electron spin-relaxation anisotropy was observed caused by a competition of the structure and bulk inversion asymmetries. It was demonstrated that such a structure design makes SIA strong enough for experimental observation of the Rashba spin-orbit splitting. An example of a reflection spectrum measured on this sample in the vicinity of the heavy-hole exciton X_{hh} is shown in Fig. 1(b). The exciton resonance is clearly seen. A rather high linewidth ~5 meV is caused by variations of the Al content during the QW growth process.

The rectangular 8-nm-wide CdTe QW with different barriers was grown on a $Cd_{0.96}Zn_{0.04}Te$ substrate in the [001] direction. The left barrier is a 90-nm-wide $Cd_{0.9}Zn_{0.1}Te$ layer, and the right barrier is a 90-nm-wide $Cd_{0.4}Mg_{0.6}Te$ layer. The details of the MBE growth can be found elsewhere [13].

We measured polarization of the light reflected from both QW structures at oblique incidence. The incident light from a halogen lamp was linearly polarized in the plane of incidence (p polarization) and perpendicular to it (s polarization). This approach has been used recently to study the optical activity of QWs [4]. The experimental geometry is shown in Fig. 1(a). The magnetic field was produced by the electromagnet with a ferromagnetic core. This allowed us to have a magnetic field up to 1 T. The closed cycle helium cryostat was placed in the core gap. The measurements were performed at temperature $T = 3$ K. The cryostat and electromagnet geometry limited the maximum incidence angle of light which in our case was $\theta_0 = 27^\circ$. All oblique incidence measurements were done at this angle. We have checked that the signal was absent at normal incidence. Spectral dependencies of the reflected light intensity $I(\omega)$ were registered by a CCD detector conjugated to a monochromator. Four polarization components of the reflected light ($I_{\sigma^\pm}$, $I_{\pm 45^\circ}$) were measured in magnetic fields from -1 to $+1$ T. Here $I_{\sigma^\pm}$ are the intensities of the reflected light in right and left circular polarizations, and $I_{\pm 45^\circ}$ are the intensities of light linearly polarized at the angle $\pm 45^\circ$ to the plane of incidence.

A direct analysis of the polarization spectra is difficult due to effects not related to MSD, e.g., birefringence. Influence of these effects are stronger than the magnetic field induced polarization conversion. For an identification of the MSD effect we used the fact that it is odd in $\boldsymbol{B}$ while the other contributions are either even or independent of the magnetic field. This allowed us to use for the analysis the differential signal measured for a fixed experimental setup and two opposite directions of the magnetic field. We analyzed the following values:

$$\rho^\pm_{\rm circ}(B) = \frac{I_{\sigma^\pm}(\boldsymbol{B}) - I_{\sigma^\pm}(-\boldsymbol{B})}{I_{\sigma^\pm}(\boldsymbol{B}) + I_{\sigma^\pm}(-\boldsymbol{B})}, \tag{2}$$

$$\rho^\pm_{\rm lin}(B) = \frac{I_{\pm 45^\circ}(\boldsymbol{B}) - I_{\pm 45^\circ}(-\boldsymbol{B})}{I_{\pm 45^\circ}(\boldsymbol{B}) + I_{\pm 45^\circ}(-\boldsymbol{B})}. \tag{3}$$

The quantities $\rho^\pm_{\rm circ}$ and $\rho^\pm_{\rm lin}$ are experimentally obtained and analyzed below. At small values of the polarization signals, $\rho^\pm_{\rm circ,lin}$ are obviously equal to the odd in $\boldsymbol{B}$ contributions to the Stokes parameters [14].

Figure 2 shows the spectral dependence of $\rho^+_{\rm circ}(\omega)$ in the GaAs triangular QW for magnetic fields from 0.05 to 1.0 T. The signal is absent in low fields. With increasing of the field, the signal arises for both X_{hh} and X_{lh} resonances being more pronounced for the latter. For $B = 1$ T, $\rho^+_{\rm circ}$ equals 0.15% at the X_{hh} line.

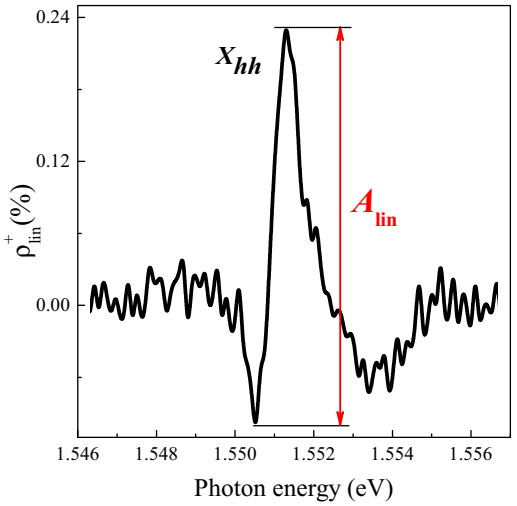

FIG. 3. Odd in $\boldsymbol{B}$ part of the linear polarization of light reflected from GaAs/AlGaAs in the vicinity of the X_{hh} resonance at magnetic field $B = 1$ T. The arrow indicates the signal amplitude plotted in Fig. 4.

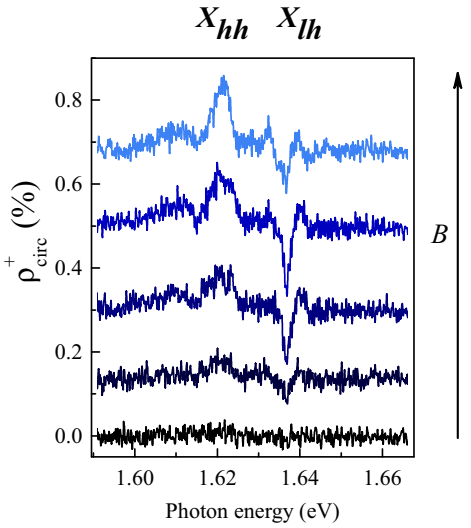

FIG. 5. Odd in $\boldsymbol{B}$ part of the circular polarization of light reflected from CdTe sample. From bottom to top: $B = 0.05$, 0.3, 0.5, 0.7, and 0.95 T.

Figure 3 shows $\rho^{+}_{\rm lin}$ at $B = 1$ T for the GaAs sample. The arrow indicates the signal amplitude $A_{\rm lin}$ which is used for the analysis of magnetic field dependencies. The value $A_{\rm circ}$ is defined in a similar way for $\rho^{+}_{\rm circ}$ [15]. The amplitudes $A_{\rm circ,lin}$ are shown in Fig. 4 for s and p polarization of the incident light. For $B > 0$ we use the data $\rho^{+}_{\rm circ,\,lin}$, and for $B < 0$ we plot $\rho^{-}_{\rm circ,\,lin}$. With a reasonable accuracy all four magnetic-field dependencies are linear. One can see that the dependencies for s and p incident polarizations are almost identical.

Experimental results for the CdTe QW show a similar behavior. Figure 5 demonstrates $\rho^{+}_{\rm circ}$ spectrum in the vicinity of X_{hh} and X_{lh} resonances. Similarly to the GaAs QW, the signal increases from 0 to 0.2% for X_{hh} with increasing of the magnetic field from 0 to 0.95 T. Figure 6 summarizes the data for $A_{\rm circ}$ and $A_{\rm lin}$ for the CdTe QW. The linear field dependence is clearly seen for the whole magnetic field range.

III. THEORY

In the present work, we study reflection from QWs in the vicinity of exciton resonances. Generally, it is described by a nonlocal integral relation between the dielectric polarization $\boldsymbol{P}(z)$ and the electric field $\boldsymbol{E}(z')$ where z is the coordinate normal to the QW plane [16]. Therefore the susceptibility $\hat{\boldsymbol{\chi}}(z,z')$ in Eq. (1) depends on both coordinates but, due to homogeneity in the QW plane, the expansion over powers of $\boldsymbol{q}_{\parallel}$ is possible. According to the experimental geometry, Fig. 1(a), where the magnetic field lies in both the QW plane and the incidence plane, $\boldsymbol{B} \parallel \boldsymbol{q}_{\parallel}$, we deal with the MSD effects caused by SIA. Phenomenologically, it means that we can consider an idealized system with the point symmetry group $C_{\infty v}$. The symmetry consideration yields for this point group that the following components of the susceptibility tensor Eq. (1) and bilinear combinations of in-plane components of $\boldsymbol{B}$ and $\boldsymbol{q}$ are

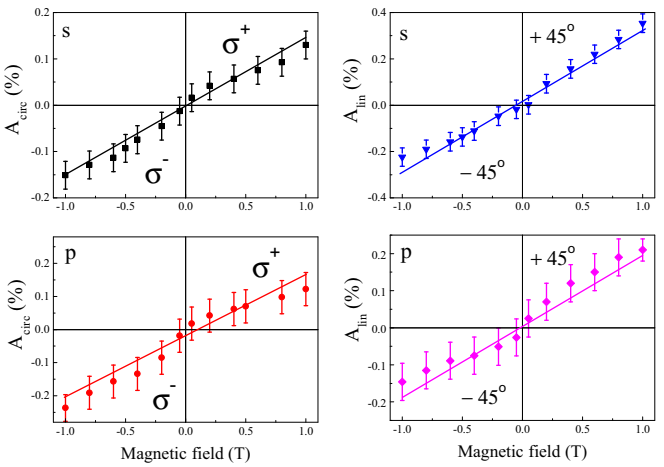

FIG. 4. Magnetic field dependencies of the signal amplitudes for GaAs/AlGaAs sample for circular and linear polarizations at s and p polarizations of the incident light.

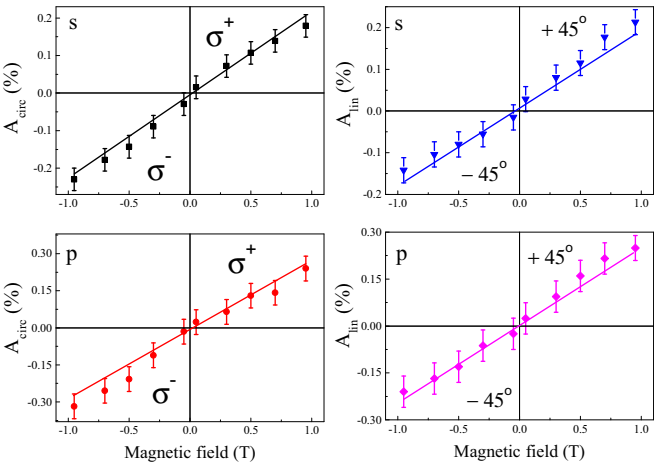

FIG. 6. Magnetic field dependencies of the amplitudes $A_{\rm circ}$ and $A_{\rm lin}$ in CdTe sample for circular and linear polarizations at s and p polarizations of the incident light.

transformed according to the same representation E_2:

$$\chi_{xy} + \chi_{yx} = C(q_x B_x - q_y B_y),$$
$$\chi_{xx} - \chi_{yy} = C(q_x B_y + q_y B_x). \quad (4)$$

Here x, y are arbitrary axes in the QW plane, and C is the single nonzero component of the four-rank tensor $\hat{\boldsymbol{C}}$ introduced in Eq. (1). Below we consider two microscopic mechanisms of MSD in structure-asymmetric QWs and calculate the value of the polarization conversion coefficient.

A. Orbital mechanism

The heavy- and light-hole states in QWs are described in the model of the Luttinger Hamiltonian [16]. Treating its off-diagonal terms as a perturbation, we obtain the wave function of the heavy hole in the ground size-quantized subband $hh1$ with the wave vector $\boldsymbol{k}$ in the QW plane in the following form:

$$\Psi^{B=0}_{hh1,\boldsymbol{k}} = C_{hh1}(z)u_{3/2} + \frac{\gamma_2\hbar^2 k_+^2}{m_0}\sum_n \frac{\phi_{lhn}(z)}{E_{hh1} - E_{lhn}}u_{-1/2}. \quad (5)$$

Here $k_+ = k_x + ik_y$, γ_2 is the Luttinger parameter, C_{hh1} and ϕ_{lhn} are the functions of size quantization of the corresponding levels of the heavy and light holes (in the absence of SIA, the functions C_{hh1} and $\phi_{lh,(2k+1)}$ are even, and $\phi_{lh,2k}$ are odd relative to the center of the QW), and u_μ are the Bloch amplitudes,

$$u_{3/2} = -\frac{X + iY}{\sqrt{2}}\uparrow, \quad u_{-1/2} = \frac{X - iY}{\sqrt{6}}\uparrow + \sqrt{\frac{2}{3}}Z\downarrow. \quad (6)$$

In the magnetic field $\boldsymbol{B}$ lying in the QW plane the component $A_+(z) = -izB_+$ is nonzero. Therefore making the Peierls substitution

$$k_+^2 \to \left(k_+ - \frac{e}{\hbar c}A_+\right)^2 \approx k_+^2 - 2k_+A_+(z), \quad (7)$$

we obtain to the linear order in the field

$$\Psi^{\boldsymbol{B}}_{hh1,\boldsymbol{k}} = C_{hh1}(z)u_{3/2} - \frac{2\gamma_2\hbar^2}{m_0}k_+\sum_n \phi_{lhn}(z)\frac{\langle lhn|A_+(z)|hh1\rangle}{E_{hh1} - E_{lhn}}u_{-1/2}. \quad (8)$$

We choose the vector potential in the form $\boldsymbol{A} = (zB_y, -zB_x, 0)$ where the point $z = 0$ is taken in the center of the QW [17]. Then we obtain

$$\Psi^{\boldsymbol{B}}_{hh1,\boldsymbol{k}} = C_{hh1}(z)u_{3/2} + iB_+k_+F(z)u_{-1/2}, \quad (9)$$

where we omit the $\boldsymbol{B}$-independent quadratic in k term,

$$F(z) = \frac{2e\gamma_2\hbar}{m_0 c}\sum_n \phi_{lhn}(z)\frac{z_{lhn,hh1}}{E_{hh1} - E_{lhn}}, \quad (10)$$

$$z_{lhn,hh1} = \int_{-\infty}^{\infty} dz\phi^*_{lhn}(z)\, z\, C_{hh1}(z). \quad (11)$$

As a result, the state with the angular momentum $3/2$ is active simultaneously in both x and y polarizations at $k \neq 0$:

$$\Psi^{\boldsymbol{B}}_{hh1,\boldsymbol{k}} = -\frac{1}{\sqrt{2}}\uparrow\left[XC_{hh1}(z) - \frac{Y}{\sqrt{3}}B_+k_+F(z)\right] - \frac{i}{\sqrt{2}}\uparrow\left[YC_{hh1}(z) - \frac{X}{\sqrt{3}}B_+k_+F(z)\right] + i\sqrt{\frac{2}{3}}B_+k_+F(z)Z\downarrow. \quad (12)$$

As a result, we obtain the terms linear in both $\boldsymbol{B}$ and $\boldsymbol{k}$ in the components of the dipole momentum density, $d_i = \langle e1\uparrow|\hat{d}_i|3/2\rangle$,

$$d_x = -\frac{ep_{cv}}{\sqrt{2}\omega_0 m_0}\langle e1|hh1\rangle(1 - i\xi B_+k_+), \quad (13)$$

$$d_y = -i\frac{ep_{cv}}{\sqrt{2}\omega_0 m_0}\langle e1|hh1\rangle(1 + i\xi B_+k_+), \quad (14)$$

where p_{cv} is the interband momentum matrix element and ω_0 is the exciton frequency. The small real parameter ξ which is nonzero due to SIA is given by

$$\xi = \frac{2e\gamma_2\hbar}{\sqrt{3}m_0 c}\sum_n \frac{z_{lhn,hh1}}{E_{hh1} - E_{lhn}}\frac{\langle e1|lhn\rangle}{\langle e1|hh1\rangle}. \quad (15)$$

Calculation of the matrix elements $\langle e1\downarrow|\hat{d}_{x,y}|-3/2\rangle$ yields analogous results.

The components of the exciton dielectric polarization satisfy the following equations [16]:

$$(\omega_0 - \omega - i\Gamma)P_x(z) = \Phi(z)\int dz'\Phi(z')[2|d_x|^2E_x(z') + (d_x^*d_y + d_y^*d_x)E_y(z')], \quad (16)$$

$$(\omega_0 - \omega - i\Gamma)P_y(z) = \Phi(z)\int dz'\Phi(z')[(d_x^*d_y + d_y^*d_x)E_x(z') + 2|d_y|^2E_y(z')]. \quad (17)$$

Here the real function $\Phi(z)$ is the envelope function of the exciton size quantization at coinciding coordinates of electron and hole, ω_0 and Γ are the heavy-hole resonant frequency and linewidth, and we ignore a small difference of the resonant frequencies and linewidths of excitons with different polarizations. We obtain from Eqs. (13)–(17) that the MSD induced contribution to the susceptibility has the form of Eqs. (4), with the nonlocal response function C given by

$$C(z,z') = \frac{\xi\nu}{\hbar}\left|\frac{ep_{cv}}{\omega_0 m_0}\right|^2|\langle e1|hh1\rangle|^2\frac{\Phi(z)\Phi(z')}{\omega_0 - \omega - i\Gamma}. \quad (18)$$

Here we take into account that the hole and the light wave vectors are related by

$$\boldsymbol{k} = \nu\boldsymbol{q}_\parallel, \quad \nu = \frac{m_h}{m_e + m_h}, \quad (19)$$

with m_h and m_e being the heavy-hole mass in the QW plane and the electron effective mass, respectively.

In the present work, we study light reflection from QWs. It is described by the reflection coefficient tensor $\hat{\boldsymbol{r}}$ relating the

light fields of the incident ($\boldsymbol{E}^0$) and the reflected ($\boldsymbol{E}^r$) waves. Solving the problem of light reflection [16], we obtain

$$\begin{pmatrix} E_s^r \\ E_p^r \end{pmatrix} = \begin{pmatrix} r_s^{QW} + \Delta r_s & \mathcal{R} \\ \mathcal{R} & r_p^{QW} + \Delta r_p \end{pmatrix} \begin{pmatrix} E_s^0 \\ E_p^0 \end{pmatrix}. \tag{20}$$

Here r_s^{QW} and r_p^{QW} are given by the standard expressions for the reflection coefficients from the QW for s and p polarized light,

$$r_s^{QW} = \frac{i\Gamma_s^0}{\omega_0 - \omega - i\Gamma}, \quad r_p^{QW} = \frac{i\left(\Gamma_p^0 - \Gamma_\parallel^0\right)}{\omega_0 - \omega - i\Gamma}, \tag{21}$$

where $\Gamma_{p,s}^0 = \Gamma_0(\cos\theta)^{\pm 1}$, $\Gamma_\parallel^0 = 4\Gamma_p^0 \tan^2\theta$, with Γ_0 being the exciton oscillator strength at normal incidence, and θ is the light propagation angle in the barrier material [16]. With account for SIA ($\xi \neq 0$), we get the MSD corrections to the reflection coefficients of s and p polarized light,

$$\Delta r_s = -2\xi\nu(q_x B_y + q_y B_x) r_s^{QW}, \quad \Delta r_p = -\Delta r_s \cos^2\theta, \tag{22}$$

as well as the polarization conversion coefficient

$$\mathcal{R} = 2\xi\nu(q_y B_y - q_x B_x)\cos\theta\, r_s^{QW}. \tag{23}$$

The polarization parameters of the reflected light observed in the experiment, Eqs. (2) and (3), are given by [4,18]

$$\rho_{\text{circ}}^{\pm} = 2\text{Im}(\mathcal{R}/r_i), \quad \rho_{\text{lin}}^{\pm} = 2\text{Re}(\mathcal{R}/r_i), \tag{24}$$

where $i = s, p$ is the incident light polarization, and r_i is the reflection coefficient from the whole structure.

B. Spin mechanism

There is another microscopic mechanism resulting in the MSD effects in QWs. It is based on $\boldsymbol{k}$-linear mixing of the heavy and light holes and the Zeeman splitting of the light-hole states. Let us take into account these two perturbations, $\mathcal{H}^{\boldsymbol{k}}$ and $\mathcal{H}^{\boldsymbol{B}}$. The first mixes the states $3/2$ and $1/2$, and the second mixes the $1/2$ and $-1/2$ states:

$$\mathcal{H}^{\boldsymbol{k}}_{1/2,3/2} = \frac{\gamma_3\sqrt{3}\hbar^2}{m_0} k_z k_+, \quad \mathcal{H}^{\boldsymbol{B}}_{-1/2,1/2} = \frac{e\hbar}{m_0 c}\varkappa B_+. \tag{25}$$

Here γ_3 and $\varkappa$ are the Luttinger parameters [16]. In the second order of perturbation theory, the wave function of the heavy hole in the $hh1$ subband with the wave vector $\boldsymbol{k}$ has the form

$$\Psi^{\boldsymbol{B}}_{hh1,\boldsymbol{k}} = C_{hh1}(z)u_{3/2} + \frac{\gamma_3\sqrt{3}e\hbar^3}{m_0^2 c}\varkappa k_+ B_+ \times \sum_n \frac{\langle lhn|k_z|hh1\rangle}{(E_{hh1} - E_{lhn})^2}\phi_{lhn}(z)u_{-1/2}. \tag{26}$$

We again obtained the hole wave function in the ground subband in the form Eq. (9), where for the spin mechanism

$$F_s(z) = -\frac{\gamma_3\sqrt{3}e\hbar^3}{m_0^2 c}\varkappa \sum_n \frac{\langle lhn|ik_z|hh1\rangle}{(E_{hh1} - E_{lhn})^2}\phi_{lhn}(z). \tag{27}$$

Therefore the spin mechanism yields the above derived Eqs. (22)–(24) for the reflection coefficients where

$$\xi_s = -\frac{e\gamma_3\hbar^3}{m_0^2 c}\varkappa \sum_n \frac{\langle lhn|ik_z|hh1\rangle}{(E_{hh1} - E_{lhn})^2}\frac{\langle e1|lhn\rangle}{\langle e1|hh1\rangle}. \tag{28}$$

IV. DISCUSSION

The light polarization conversion is detected and analyzed in the vicinity of the heavy-hole exciton X_{hh}. It is shown that the signal is linear in the in-plane magnetic field in both GaAs- and CdTe-based QWs. For effects linear in the magnetic field, the obvious relationship takes place:

$$\rho^{+}_{\text{circ, lin}}(B) = -\rho^{-}_{\text{circ, lin}}(B). \tag{29}$$

Our experimental data demonstrate that this relation is fulfilled in our experiments with a high accuracy. Indeed, Figs. 4 and 6 clearly show that the experimental data for two orthogonal polarizations lie on the same linear dependence on the magnetic field.

Theoretical consideration shows that the X_{hh} state has zero dipole momentum along the growth direction z, which forbids the MOKE at X_{hh}. In contrast, MSD makes the the polarization conversion possible. Microscopically, for an oblique light incidence, the exciton as a whole has a finite wave vector $\boldsymbol{q}_\parallel$ in the QW plane. This results in the off-diagonal terms in the matrix of reflection coefficients (20).

In order to experimentally discriminate between MSD and MOKE we note that the MSD contribution to the polarization conversion is given by equal off-diagonal coefficients $r_{sp}^{\text{MSD}} = r_{ps}^{\text{MSD}} = \mathcal{R}$ in Eq. (20) while for MOKE they are opposite in sign: $r_{sp}^{\text{MOKE}} = -r_{ps}^{\text{MOKE}}$. This allows us to separate MSD and MOKE contributions analyzing the sum and the difference of the conversion signals obtained at s and p polarizations of the incident light:

$$\rho_{\text{circ}}^{\text{MSD}} = \frac{\rho_{\text{circ}}^{(p)} + \rho_{\text{circ}}^{(s)}}{2}, \quad \rho_{\text{circ}}^{\text{MOKE}} = \frac{\rho_{\text{circ}}^{(p)} - \rho_{\text{circ}}^{(s)}}{2}. \tag{30}$$

Here $\rho_{\text{circ}}^{(p/s)}$ is the circular polarization of the reflected light ρ_{circ}^{+} at incidence of p/s polarized light. We relate $\rho_{\text{circ}}^{(p/s)}$ with r_{sp} and r_{ps} by Eq. (24) neglecting a difference in the reflection coefficients from the whole structure r_s and r_p. We have checked that the account for their difference at an incidence angle $\theta_0 = 27^\circ$ is about 20% which does not affect the analysis strongly. We analyzed the circular polarization of the reflected light because it is determined with higher accuracy in our setup.

The extracted from experiment MSD and MOKE contributions $\rho_{\text{circ}}^{\text{MSD}}$ and $\rho_{\text{circ}}^{\text{MOKE}}$ are plotted in Fig. 7. It is seen that MSD is present at X_{hh} and MOKE is absent while both MSD and MOKE signals exist at X_{lh}. However MSD dominates even at X_{lh} resonance. A weak MOKE signal can be related with a small Zeeman splitting of the X_{lh} state. Experimental data presented in Fig. 7 demonstrate that the polarization conversion at the heavy-hole exciton is caused by the magnetospatial dispersion effect in QWs.

The above conclusion allows analyzing the experimental data based on the developed theory of MSD in QWs. Theoretical consideration performed in the previous section demonstrates that the polarization conversion spectrum $\mathcal{R}(\omega)$

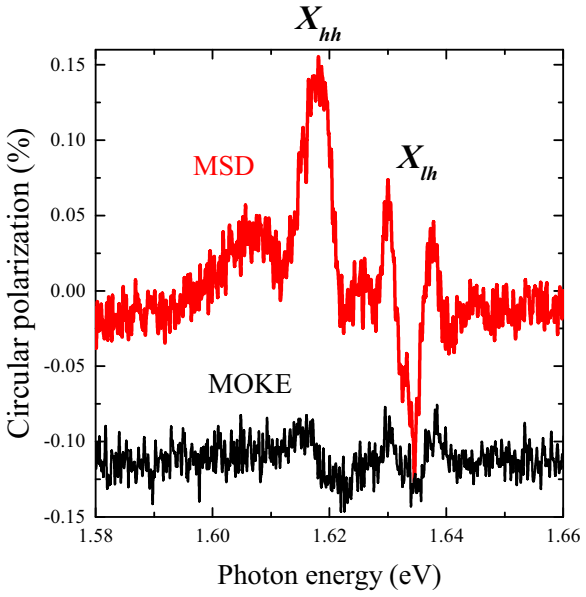

FIG. 7. MSD and MOKE contributions to the circular polarization of light reflected from CdTe sample in the magnetic field $B = 0.95$ T.

has a resonance near the X_{hh} exciton, Eqs. (21) and (23). This resonant behavior is clearly seen in Figs. 2, 3, and 5.

The developed theory shows that the MSD contribution to the polarization conversion is controlled by SIA. The orbital and spin mechanisms yield additive contributions to MSD which are proportional to the parameters ξ and ξ_s, Eqs. (15) and (28). If the QW is structure-symmetric then for odd $n = 1,3,5\ldots$ the coordinate and momentum matrix elements, $z_{lhn,hh1}$ and $\langle lhn|k_z|hh1\rangle$, are zero while for even $n = 2,4,\ldots$ the overlap of the electron and light-hole envelope functions $\langle e1|lhn\rangle$ is zero. Therefore the parameters ξ and ξ_s are present in QWs with SIA only, and they change signs, for example, at a reversal of the normal electric field applied to a symmetric QW. It follows from the developed microscopic theory that the orbital and spin contributions to MSD are related by

$$\left|\frac{\xi_s}{\xi}\right| \sim \varkappa\frac{m}{m_0}, \tag{31}$$

where m has an order of the hole mass for the motion along the growth direction. Since for both GaAs and CdTe the product $\varkappa m/m_0 \approx 0.3$ [19], the spin and orbital mechanisms give comparable contributions to MSD, but the orbital one is a little stronger for both GaAs and CdTe QWs.

We can estimate the SIA parameter as $\xi \sim (e/\hbar c)a^2 z_{lh1,hh1}$, where a is the hole localization length in the QW structure; see Eq. (15). For $a = 8$ nm we get $\xi \sim (z_{lh1,hh1}/a)$ nm T^{-1}. The MSD effect in reflection is the polarization conversion coefficient $\mathcal{R} \approx \xi q_\parallel B$. This yields for $q_\parallel \sim 4\times10^4$ cm^{-1} an estimate $\mathcal{R}/B \sim 0.005(z_{lh1,hh1}/a)$ T^{-1}. Let us compare this theoretical estimate with experiment. Experimental results presented in Figs. 4 and 6 show the amplitude of MSD signal in both GaAs- and CdTe-based QWs is $\sim10^{-3}B$ T^{-1}. This corresponds to the 20% SIA degree in both QWs: $z_{lh1,hh1}/a \sim 0.2$. This is a reasonable estimate for both structures. In the 8-nm-wide CdTe QW under study, SIA is caused by the difference in the left and right barrier materials. This difference results in a shift of the hole wave functions from the point in the middle of the QW and, hence, to a nonzero matrix element $z_{lh1,hh1}$. In the GaAs QW the right barrier height increases smoothly from zero to the left barrier height value at a width 27 nm; see Sec. II. As a result, both localization length a and SIA degree are larger than in the CdTe QW. This explains the comparable polarization conversion coefficients in GaAs and CdTe QWs.

V. CONCLUSION

The magnetospatial dispersion is demonstrated in both III-V and II-VI QWs. The MSD induced conversion of the light polarization state is observed in the magnetic fields $B \leqslant 1$ T. The polarization conversion signal increases linearly with B and reaches the values 2×10^{-3} at $B = 1$ T in both studied samples. The developed theory based on the in-plane wave vector and magnetic field induced mixing of the heavy- and light-hole states explains the measured signal assuming a reasonable 20% degree of SIA. As an outlook, the geometry of in-plane magnetic field perpendicular to the incidence plane will be investigated. The corresponding studies allow us to determine a degree of the bulk inversion asymmetry which results in the magnetospatial dispersion in this case.

ACKNOWLEDGMENTS

We thank M. M. Glazov for fruitful discussions. Optical measurements performed by L.V.K. were supported by Russian Science Foundation (Project No. 16-12-10503). L.E.G. thanks Russian Science Foundation (Project No. 14-12-01067) for support of his theoretical work and "BASIS" foundation.

[1] A. K. Zvezdin and V. A. Kotov, *Modern Magnetooptics and Magnetooptical Materials* (Institute of Physics Publishing, Bristol, 1997).

[2] V. M. Agranovich and V. L. Ginzburg, *Crystal Optics with Spatial Dispersion and Excitons* (Springer, Berlin, 1984).

[3] S. D. Ganichev and L. E. Golub, Interplay of Rashba/Dresselhaus spin splittings probed by photogalvanic spectroscopy—A review, Phys. Status Solidi B **251**, 1801 (2014).

[4] L. V. Kotova, A. V. Platonov, V. N. Kats, V. P. Kochereshko, S. V. Sorokin, S. V. Ivanov, and L. E. Golub, Optical activity of quantum wells, Phys. Rev. B **94**, 165309 (2016).

[5] O. V. Gogolin, V. A. Tsvetkov, and E. G. Tsitsichvili, Magnetically induced birefringence in cubic crystals, Sov. Phys. JETP **60**, 593 (1984).

[6] E. L. Ivchenko, V. P. Kochereshko, G. V. Mikhailov, and I. N. Uraltsev, Resonance magneto-spatial dispersion of crystals, Phys. Status Solidi B **122**, 221 (1984).

[7] B. B. Krichevtsov, R. V. Pisarev, A. A. Rzhevskii, and H. J. Weber, Manifestation of magnetically induced spatial dispersion in the cubic semiconductors ZnTe, CdTe, and GaAs, JETP Lett. **69**, 551 (1999).

[8] T. Godde, M. M. Glazov, I. A. Akimov, D. R. Yakovlev, H. Mariette, and M. Bayer, Magnetic field induced nutation of exciton-polariton polarization in (Cd, Zn)Te crystals, Phys. Rev. B **88**, 155203 (2013).

[9] V. Kochereshko, V. Kats, A. Platonov, V. Sapega, L. Besombes, D. Wolverson, and H. Mariette, Nonreciprocal magneto-optical effects in quantum wells, Phys. Status Solidi C **11**, 1316 (2014).

[10] B. B. Krichevtsov, R. V. Pisarev, A. A. Rzhevsky, V. N. Gridnev, and H.-J. Weber, Magnetospatial dispersion effect in magnetic semiconductors $Cd_{1-x}Mn_xTe$, Phys. Rev. B **57**, 14611 (1998).

[11] M. Lafrentz, D. Brunne, A. V. Rodina, V. V. Pavlov, R. V. Pisarev, D. R. Yakovlev, A. Bakin, and M. Bayer, Second-harmonic generation spectroscopy of excitons in ZnO, Phys. Rev. B **88**, 235207 (2013).

[12] N. S. Averkiev, L. E. Golub, A. S. Gurevich, V. P. Evtikhiev, V. P. Kochereshko, A. V. Platonov, A. S. Shkolnik, and Yu. P. Efimov, Spin-relaxation anisotropy in asymmetrical (001) $Al_xGa_{1-x}As$ quantum wells from Hanle-effect measurements: Relative strengths of Rashba and Dresselhaus spin-orbit coupling, Phys. Rev. B **74**, 033305 (2006).

[13] W. Grieshaber, J. Cibert, J. A. Gaj, Y. M. d'Aubigné, and A. Wasiela, Profiles of the normal and inverted semiconductor interfaces: A Zeeman study in asymmetric $Cd_{1-y}Zn_yTe$/CdTe/$Cd_{1-x}Mn_xTe$ quantum wells, Phys. Rev. B **50**, 2011(R) (1994).

[14] M. Born and E. Wolf, *Principles of Optics* (Pergamon, Oxford, 1970).

[15] For the spectrum shown in Fig. 3 we define $A_{\rm lin} > 0$. At an opposite phase of the spectrum $\rho^{\pm}_{\rm lin,\,circ}(\omega)$ the amplitudes are defined with the negative sign.

[16] E. L. Ivchenko, *Optical Spectroscopy of Semiconductor Nanostructures* (Alpha Science Int., Harrow, UK, 2005).

[17] Despite that the wave function depends on the vector potential which can be shifted by an arbitrary constant $\boldsymbol{A}(z) \to \boldsymbol{A}(z) + \boldsymbol{A}_0$, one can see that such a shift is equivalent to the substitution $\boldsymbol{k} \to \boldsymbol{k} - (e/\hbar c)\boldsymbol{A}_0$. This shift in the $\boldsymbol{k}$ space does not change measurable quantities.

[18] D. S. Smirnov and M. M. Glazov, Stochastic Faraday rotation induced by the electric current fluctuations in nanosystems, Phys. Rev. B **95**, 045406 (2017).

[19] M. V. Durnev, Zeeman splitting of light hole in quantum wells: Comparison of theory and experiments, Phys. Solid State **56**, 1416 (2014).